Materials and Structures
DOI 10.1617/s11527-012-9950-y

ORIGINAL ARTICLE

Numerical modeling of the rebar/concrete interface: case of the flat steel rebars

T. S. Phan · J.-L. Tailhan · P. Rossi · Ph. Bressolette · F. Mezghani

Received: 23 September 2011 / Accepted: 27 September 2012

Abstract This paper presents the methodology used to identify the mechanical behaviour of a steel-concrete interface in the case of a particular steel reinforcement (flat steel). The methodology consists in simulating the statistical mechanical behaviour of reinforced concrete tie-beams, subjected to tension, using a probabilistic discrete approach for the mechanical behaviour of the concrete under axial tension and a deterministic model for the steel-concrete interface. The model proposed for the interface is in the frame of damage mechanics taking into account physical phenomena related to the interface (cohesion and slip). The tie-beams are reinforced by a flat steel rebar with a rectangular cross section of 25 × 3.5 mm. Results of this numerical simulation have been compared to some experimental tests results. These comparisons are performed in terms of global responses (load-displacement curves) and of local responses (crack openings, number of cracks and cracks' spacing).

T. S. Phan (✉) · J.-L. Tailhan · P. Rossi
Paris-Est University, IFSTTAR, 58 boulevard Lefebvre, 75732 Paris CEDEX 15, France
e-mail: thanh-song.phan@ifsttar.fr; phan.thanhsong@yahoo.com

Ph. Bressolette
Clermont University, Blaise Pascal University LaMI, EA3867, BP 206, 63000 Clermont, France

F. Mezghani
Màtiere-Construction Company, BP 54, 15130 Arpajon-sur-Cère, France

Published online: 12 October 2012

Keywords Reinforced concrete · Flat steel · Steel-concrete interface · Cracking

List of symbols

f_c	Compressive strength of concrete (MPa)
f_t	Tensile strength of concrete (MPa)
E_c	Young's modulus of concrete (MPa)
D_g	Diameter of largest aggregate in concrete (m)
V_S	Volume of the finite element (m^3)
V_A	Volume of the largest aggregate (m^3)
$m(X)$	Mean value of X (MPa)
$\sigma\ (X)$	Deviation value of X (MPa)
F_{mX}	Mean function of X
$F_{\sigma\ X}$	Deviation function of X
E_s	Young's modulus of steel (MPa)
R_e	Yield strength of steel (MPa)
R_u	Ultimate strength of steel (MPa)
C	Cohesion of interface (MPa)
δ_t^{cri}	Critical tangential displacement (m)
δ_t^e	Threshold tangential displacement (m)
δ_t	Relative tangential displacement (m)
δ_n^{cri}	Critical normal displacement (m)
δ_n^e	Threshold normal displacement (m)
δ_n	Relative normal displacement (m)
σ_n	Normal stress (MPa)
τ	Tangential stress (MPa)
ϕ	Friction angle (°)
ψ	Dilatancy angle (°)
K	Stiffness matrix of contact element
d_0	Previous damage state
d	Damage state

w Crack opening (m)
e Fictive elastic interface thickness (m)

1 Introduction

For developing a new technological solution of reinforcement for RC structures, it is primordial to understand and identify the main physical mechanisms involved especially when numerical simulation tools are used to demonstrate the mechanical efficiency of this new solution.

The construction company MATIERE® has developed and patented, in recent years, a new type of flat steel reinforcement. It can be used in structural elements and shows some advantages: (1) reduction of the total thickness of the structure by reducing the thickness of the steel, (2) decrease in the quantity of steel by using tendrils replacing the anchorages of steel round rebars, (3) increase in surface of adhesion, (4) easy of implementation, welding, ... Mechanically speaking the main difference between this new type of steel reinforcement and the traditional one (cylindrical rebars) concerns the interface behaviour between the flat steel and the concrete. In consequence, the modeling of this interface behaviour has to be taken in account for a relevant analysis of the behaviour of the structure reinforced with this type of steel reinforcement.

In this paper, the modeling of a tie-beam reinforced by flat steel and subjected to axial tension is presented. The study is mainly focused on the mechanical effect of the steel-concrete interface on the cracking process of the tie-beams. The behaviour of the concrete under axial tension is taking into account by using a probabilistic discrete cracking model [1, 2], which integrates the heterogeneity of the material, scale effects, and gives an explicit representation of the cracks in the concrete. The steel-concrete interface is represented by classical interface elements. Their behaviour is described by a simple deterministic damage mode. This model macroscopically takes into account the main physical phenomena of the interface through only two parameters: a cohesion and a slip (i.e. tangential relative displacement between steel and concrete).

The originality of this work is to propose an integrated approach in which the modeling of the steel/concrete interface takes into account the manner how the concrete cracking is modeled (macroscopic approaches for the concrete and the interface modelings). As a matter of fact, the modeling of this interface is consistent with the fact that the concrete cracking is describe through the use of a probabilistic discrete cracking model (see Fig. 2). In others words, the modeling chosen for the interface is directly limited to the concrete cracking modeling and has no general relevancy.

In this way, an inverse analysis approach is used to identify the parameters of the interface behaviour. The numerical results are compared with those of the experimental ones. This comparison is made in terms of global response (load vs. relative displacement), as well as local information (cracks opening, cracks spacing and number of cracks). Some factors related to the implementation of the reinforcement in the concrete (eccentricity of steel, structure of concrete around the steel) are also emphasized.

2 Modeling strategy

In the literature, there are many explanations concerning the mechanical deterioration of the steel-concrete interface. But the one proposed by Tassios [3] is the most commonly adopted. Findings of this research indicate that the activation process of the steel-concrete interface of a pull-out test has four phases during loading:

- A linear behaviour of the interface until the break of the adhesion,
- A slip-friction behaviour until a maximum slip,
- A phase of constant shear,
- The destruction of the interface.

However, the cracking process can be complex and depends on many parameters [4] related to concrete (concrete quality, coating ...) and steel (diameter, type of notches, indentations). Similar observations are obtained in the case of tests on flat steels.

In this paper, the modeling of a tie-beam test under axial tension is presented. The objective is to determine the values of the parameters involved in the choosen modeling of the steel-concrete interface. By "coupling" this interface model with a concrete cracking one, the following information can be reached:

- Global behaviour: load-displacement of the steel,

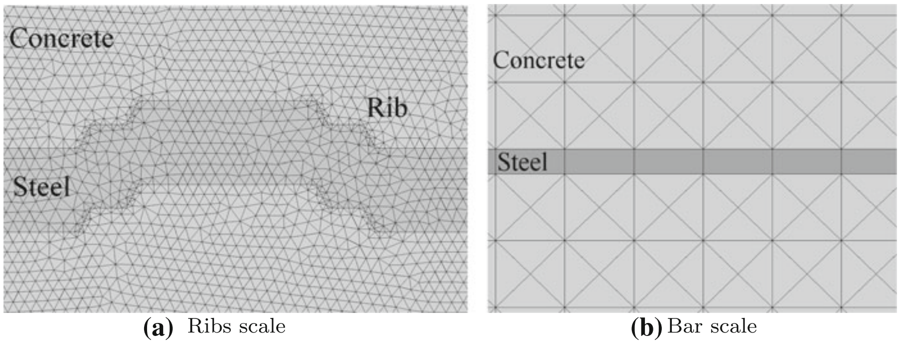

Fig. 1 Scale of steel-concrete interface

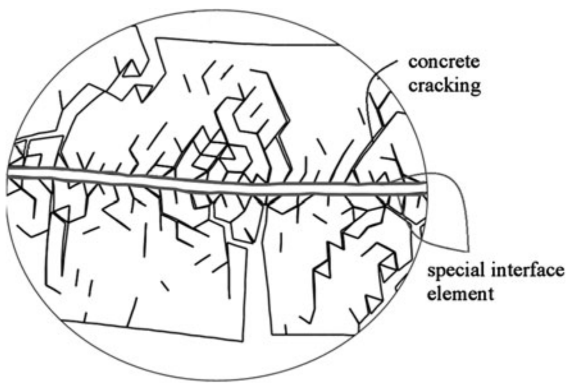

Fig. 2 Modeling of the steel-concrete interface by using interface element (focus related to a RC tie-beam subjected to tension)

- Local information: evolution of the cracks number, spacing and cracks opening during the test.

Only finite elements modeling can provide access to information both at local and global levels. In the framework of this approach, the concrete is taken into account through a probabilistic discrete cracking model. For the steel-concrete interface, two possibilities exist in relation with the scale adopted for the modeling of the cracking processes in the concrete (see paragraph 3):

- The modeling is situated at the level of the ribs of the steel (Figs. 1a, 6). The behaviour of the interface is, therefore, related to the cracking of the concrete in the neighborhood of these ribs. Some interesting examples of ribs-scale analyses are mentioned in the works of Ozbolt and Eligehausen [5], Cox and Herrmann [6], Rots [7], Reinhardt et al. [8].
- The modeling is situated on a larger scale than the one of the ribs of the steel. Therefore the ribs are not taken into account explicitly in the modeling (Fig. 1b). Some research on this scale has been made by Lundgren [9], Cox [10]. The steel-concrete interface is then described by using an interface element without thickness taking into account concrete cracking near the ribs.

The first kind of modeling leads to adopt a greater refinement of the mesh and thus will lead to very long

Fig. 3 Probabilistic concrete cracking model

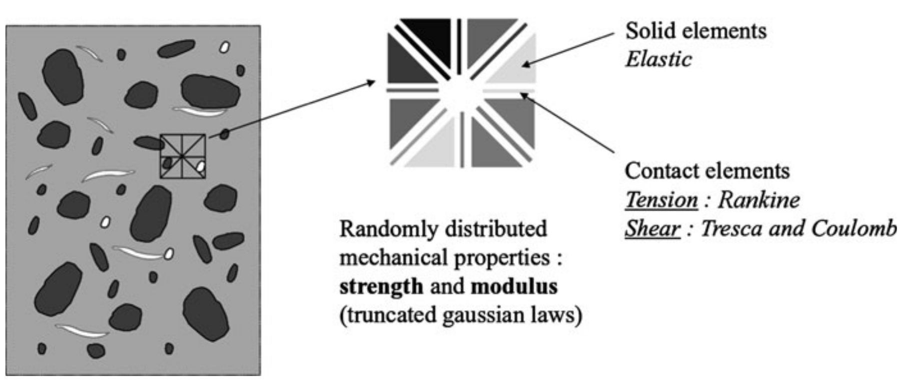

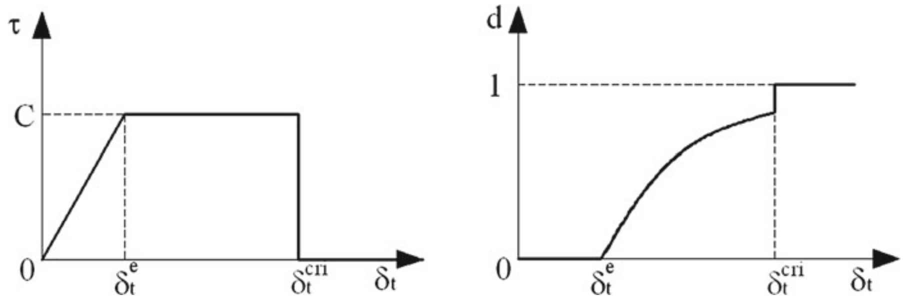

(a) Tangential stress-relative displacement relation

(b) Damage evolution

Fig. 4 Behaviour law before the failure

Fig. 5 Criteria used before failure and after failure

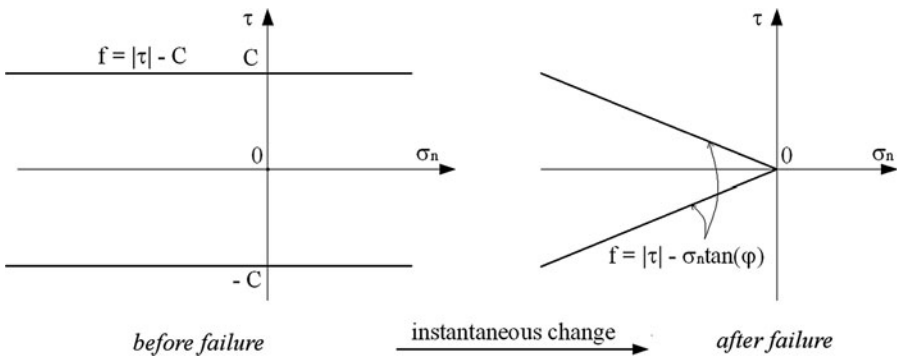

computation time. The second option is adopted in the present work. Figure 2 (example of numerical result) illustrates the scale adopted and the cracking process described.

3 Presentation of the probabilistic concrete cracking model

The behaviour of the concrete under axial tension is represented by an explicit probabilistic cracking model initially developed at IFSTTAR[1] (formerly LCPC[2]) by Rossi et al. [1]. This model has the particularity to take into account two major characteristics of concrete: heterogeneity, on the one hand, and its sensitivity to scale effects, on the other hand [2]. The concrete heterogeneity, due to its mix design, is taken into account by the fact that the local mechanical characteristics (Young's modulus E_c, tensile strength f_t) are randomly distributed and dependent on the volume of material stressed (see Fig. 3). In that way, scale effects are also a consequence of the heterogeneity of the material. As a matter of fact, the local mechanical response of the material directly depends on the volume of material stressed (in tension). Finally, the cracking process is mainly controlled by the heterogeneity of the material and the development of tensile stress gradients.

In terms of numerical modeling, these features can be summarized as follows:

- The model is based on the finite elements method, in which each finite element represents a given volume of (heterogeneous) material.
- For a given concrete (mechanically characterized by its compressive strength), the mechanical properties, such as the Young's modulus and the tensile strength, are initially randomly distributed over all elements of the mesh, using a probabilistic distribution whose characteristics depend on the ratio between the volume of the finite element and the volume of the largest aggregate (V_S/V_A):

[1] IFSTTAR—The French institute of science and technology for transport, development and networks.

[2] LCPC—French Public Works Laboratory.

Fig. 6 An example of flat steel with ribs on the surface tested by MATIERE®

$$m(X) = F_{mX}(V_S/V_A, f_c) \quad \text{and} \quad \sigma(X) = F_{\sigma X}(V_S/V_A, f_c) \tag{1}$$

where X represents either the tensile strength or the Young's modulus, $m(X)$ and σ (X) are the mean value and the standard deviation of X respectively. Note that, according to the finding of Rossi, the mean value of the Young's modulus is not affected by scale effects. This author proposes different expressions for F_{mX} and $F_{\sigma\ X}$ in [2].

- The cracks are explicitly represented by interface elements of zero thickness. These elements interface all the volume elements. The cracking criterion is very simple. It is a Rankine one in tension and a Tresca–Coulomb one in shear. Once a interface element is broken, its behaviour follows a Coulomb's law.
- Once a interface element opens, its tensile and shear strengths become equal to zero.
- Note that in this model, the cracking creation and propagation is the results of the creation of elementary failure planes that randomly appear and can coalesce to form macroscopic cracks.

4 Presentation of the steel-concrete interface model

Many studies have been performed to simulate the behaviour of RC structures taking into account the behaviour of the steel-concrete interface (models based on the plasticity theory [11–13], the damage theory [14–16] or other model [17–19]. But very few of them were focused on the role of this interface in the cracking process of the concrete. In this section, a simple and robust interface model is presented. It takes into account the nonlinear behaviour of the steel-concrete interface in the framework of damage mechanics and thermodynamics of irreversible processes. It can also take into account physical phenomena of steel-concrete interface such as interface sliding, cracks appearance and degradation process.

The interface is modeled by using the same type of element as the one used for the cracking concrete model. The role of this interface element (between steel and concrete) is:

- To ensure the displacement continuity between the concrete and the steel before the interface slipping (i.e. tangential relative displacement) and before the concrete cracking. So, it ensures the transfer of the load (and therefore of stresses) between steel and concrete.
- To model the macroscopic mechanical effect at the ribs level (which are not explicitly represented in the mesh).

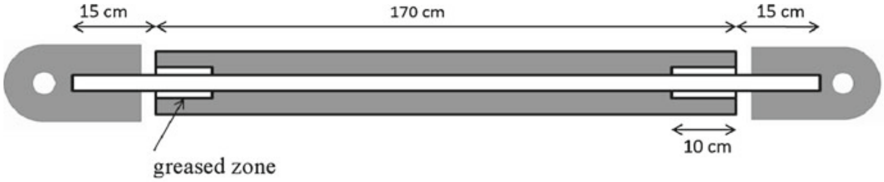

(a) Tie-beam geometry

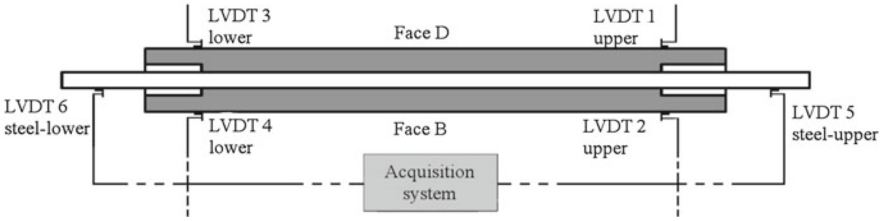

(b) Experimental device (position of LVDT sensors)

Fig. 7 Tie-beam (170 × 10 × 10 cm) reinforced by flat steel (25 × 3.5 mm)

Fig. 8 Tie-beam test—general view

Table 1 Composition of the concrete (per m^3)

Constituents	Weight in kg
Sand 0/4	743
Gravel 4/10	340
Gravel 10/16	752
Ciment CEMI 52.5 PMES	400
Superplasticizer	2.6
Water	165
Total	2402.6

Table 2 Material characteristics considered in the numerical simulations

Material	Parameters	Notation	Values	Unit
	Compressive strength	f_c	53	MPa
Concrete[a]	Young's modulus	E_c	32,000	MPa
	Maximum aggregate size	D_g	0.016	m
Flat steel	Young's modulus	E_s	200,000	MPa

[a] The tensile strength f_t of the concrete is directly calculated in the frame of the use of the probabilistic concrete cracking model (see paragraph 3)

Table 3 Characteristic parameters of crack (Numerical 2D–3D Test)

	Experiment (3D)	Modeling (2D)
Relative displacement	Average between the faces B and D	Average on the cracked faces
Number of cracks	Average over the top and bottom faces	
Cracks opening		
Cracks spacing		

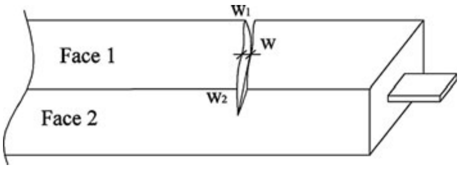

Fig. 9 Determination of the cracks opening

- To simulate a local failure between steel and concrete along the rebar if a shear cracking occurs and leads to a loss of local adhesion.
- To simulate the local friction between concrete and steel after the interface failure.

4.1 Bases of the model

In this study, the model is implemented in 2D (3D implementation is still in progress) and based on the concept of intensity of adhesion, first introduced by Frémond [20, 21]. It considers the steel-concrete interface as a material zone that progressively degrades in shear (the tensile failure is neglected). During this degradation, and before the total failure of the interface, stresses are considered to be still transmitted to the concrete.

For a sake of simplicity, a very simple approach based on a damage model is chosen. This approach allows the maintain of a constant level of stress when the critical shear is reached (see Fig. 4a). When the relative tangential displacement between the concrete and the steel exceeds a critical value, the interface element is considered as broken [22]. After the failure, a friction behaviour of Mohr-Coulomb's type is considered.

The model of the steel/concrete interface is considered as deterministic. This choice is justified by the

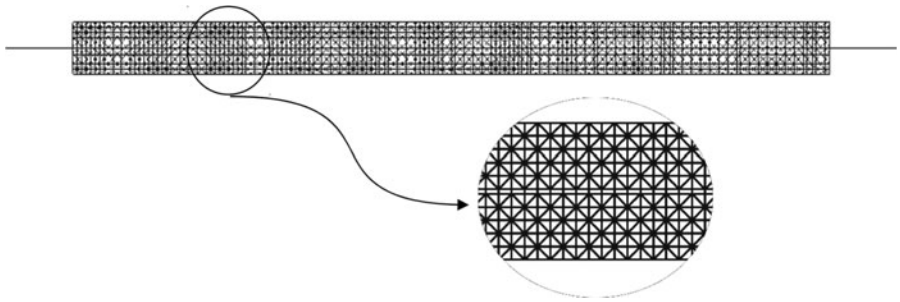

Fig. 10 Simulation of the tie-beam test 170 × 10 × 10 cm

Table 4 Material characteristics considered in the numerical simulations

Model	Elements	Parameters	Values	Unit
Cracking of concrete	8750	f_c	53	MPa
		E_c	32,000	MPa
		D_g	0.016	m
Steel-concrete interface	340	C	(10, 15, 20, 25, 30)	MPa
		δ_t^{cri}	(δ_t^e, 3, 6, 10, 30)	10^{-6} m
Flat steel (elastic)	200	E_s	210,000	MPa

fact that the cracking along the bar is spreaded due to the presence of the steel ribs (no influence of the weakest link like in Weibull theory).

The constitutive relations of the model can be briefly summarized by:

$$\begin{bmatrix} \sigma_n \\ \tau \end{bmatrix} = (1-d)K\begin{bmatrix} \delta_n \\ \delta_t \end{bmatrix} \quad \text{with,} \quad \mathrm{K} = \begin{bmatrix} \mathrm{k_n} & 0 \\ 0 & \mathrm{k_t} \end{bmatrix} \tag{2}$$

where σ_n, τ are the normal and tangential stresses, d is the damage parameter, δ_n, δ_t are the normal and tangential displacements respectively and K the stiffness matrix of the contact element.

The role of the elemental stiffness matrix is to ensure the continuity between opposite nodes and the non-interpenetration of the two bodies in contact, it is a penalty matrix. The parameters k_n and k_t of this stiffness matrix are related to the elastic modulus of the infilling material divided by the fictive elastic interface thickness e.

$$k_n = \frac{E}{e} \quad \text{and} \quad \mathrm{k_t} = \frac{\mathrm{G}}{\mathrm{e}} \tag{3}$$

In this Eq. (3), the fictive interface thickness e is estimated from a penalty coefficient which has a significant influence on the conditioning of the stiffness matrix. Therefore its value must be chosen by numerical experiments to obtain a good performance of the contact elements and a good convergence of algorithms of contact. For this type of simulation, the value of e is choosen as 10^{-6}. This choice is based on the recommandation of some finite element codes, for example CESAR (LCPC-France) [23] or Code Aster (EDF-France) [24]. This value can be found "implicitly" also in the research of Lundgren [9].

The damage evolution relation (as depicted Fig. 4b) is given by:

$$\begin{cases} d = 0 & \\ d = 1 - \frac{\delta_t^e}{|\delta_t|} & \text{if} \\ d = 1 & \end{cases} \begin{matrix} |\delta_t| < \delta_t^e \\ \delta_t^e \le |\delta_t| < \delta_t^{cri} \\ |\delta_t| \ge \delta_t^{cri} \end{matrix} \tag{4}$$

$$\delta_t^e = \frac{C}{k_t} \tag{5}$$

where δ_t^{cri} is the threshold of tangential elastic displacement, δ_t^{cri} is the critical tangential displacement ($\delta_t^{cri} \ge \delta_t^e$), and $|\delta_t|$ is the parameter which drives the evolution of damage.

In order to verify the positiveness of the thermodynamic dissipation, the damage can only increase. As a consequence, this can be summarized as:

$$\begin{cases} \dot{d} \ge 0 \\ d = max(d_0, d) \end{cases} \tag{6}$$

where d_0 is an initial damage state, and d is the actual damage state.

After the failure, when $\delta_t > \delta_t^{cri}$ and $d = 1$, a friction behaviour is considered and a Mohr-Coulomb type criterion is applied (Fig. 5). In that case, an associated flow rule g is also used (Eq. 7):

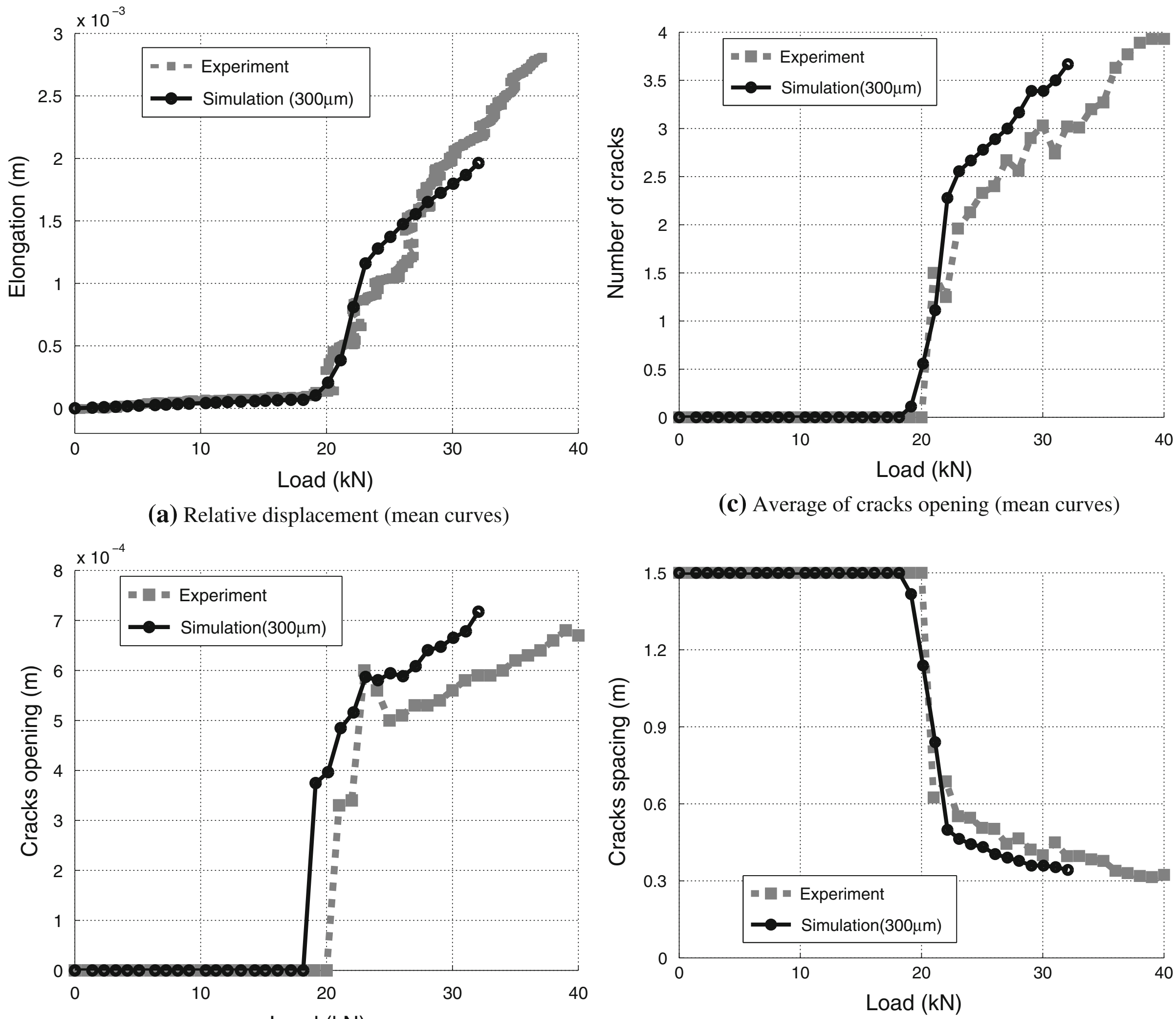

(a) Relative displacement (mean curves)

(c) Average of cracks opening (mean curves)

(b) Average of cracks opening (mean curves)

(d) Average of cracks opening (mean curves)

Fig. 11 Comparisons related to the mean values (experiments with numerical simulations)

$$\begin{cases} g = |\tau| - \sigma tan\psi \\ tan\psi = tan\phi \end{cases} \tag{7}$$

where ψ the dilatancy angle and ϕ the friction angle. Without any further information concerning ϕ and ψ and considering that the failure essentially occurs in the concrete surrounding the steel, a value of 30° is retained (value obtained from Rossi [22]).

In this study, only the values of the maximum shear stress, C, and the tangential critical relative displacement, δ_t^{cri}, have to be determined. This identification is made by an inverse approach based on a comparison between numerical and experimental results. In consequence, this determination is available only for a given rebar geometry and a given concrete.

5 Modeling of the tie-beam test: use of a flat steel

In this section, the tie-beam tests are first presented. Figure 6 shows an example of the ribs on a flat steel studied in these tests. Then, in a second step, the comparison between numerical simulations (with different values of the parameters C and δ_t^{cri}) and experimental ones are presented.

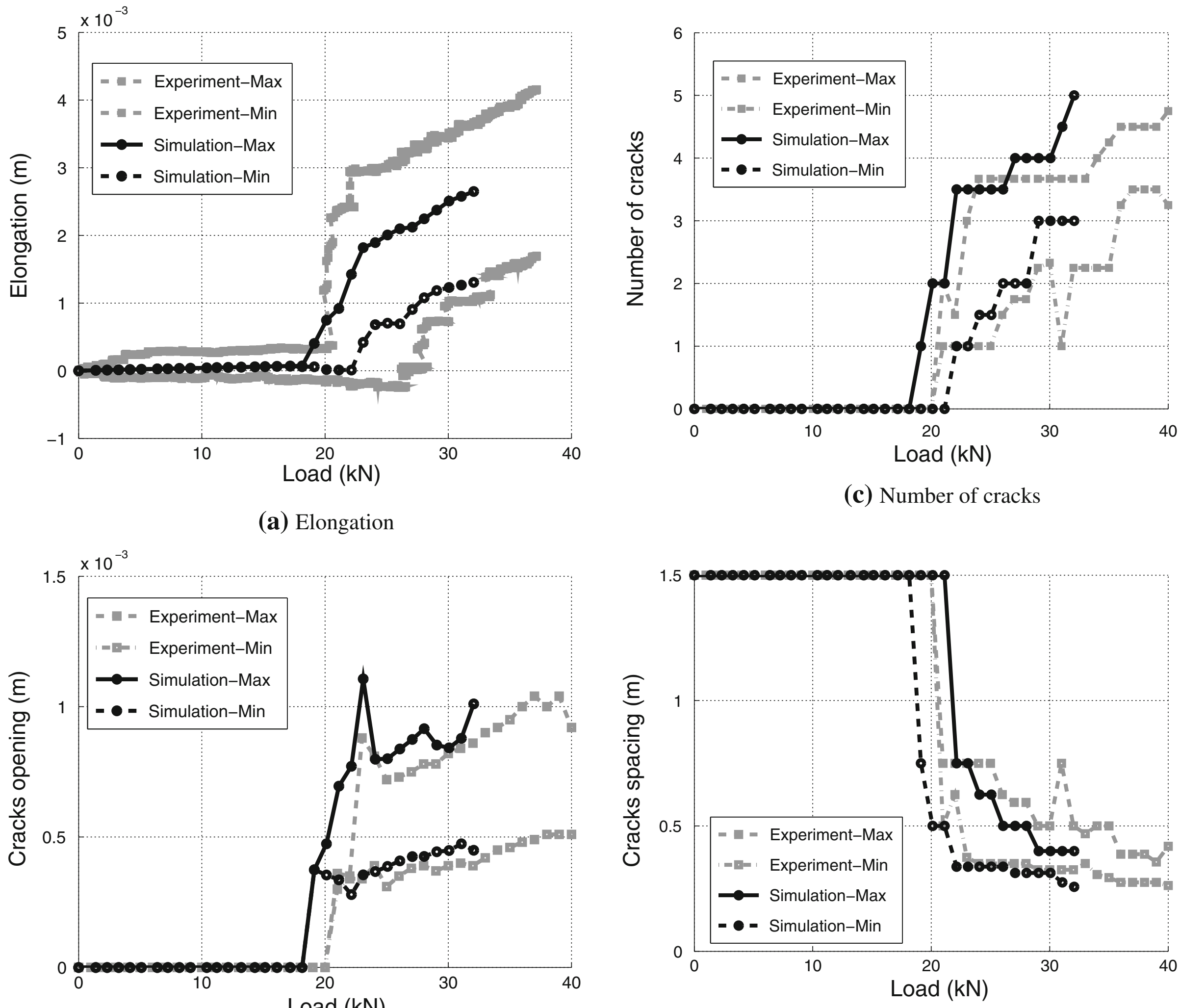

(a) Elongation

(c) Number of cracks

(b) Cracks opening

(d) Cracks spacing

Fig. 12 Scatterings related to elongations and cracks opening versus load curves (experiments and numerical simulations)

5.1 Presentation of the tie-beam test

The experimental tests on tie-beams were conducted in the laboratory of Polytech Clermont-Ferrand (Blaise Pascal University of Clermont—Ferrand, France). In these tests, the reinforced concrete tie-beams are subjected to pure tension. The dimensions of the concrete prismatic specimens are: 170 × 10 × 10 cm. The reinforcement is a flat steel with a rectangular cross section of 25 × 3.5 mm. The steel rebar is centered in the middle of the tie-beam. To minimize edge effects in the concrete during the test, “no anchor zones” of 10 cm length are considered at each extremity (Fig. 7a).

Figure 7b schematizes the experimental device and Figure 8 shows a general view.

To mesure the elongations of the concrete and the steel, six displacement sensors (linear variable differential transformers—LVDTs) are placed on the specimen (Fig. 7b). These LVDTs are fixed on a common undefor

- For the measure of the global elongation (including the steel):

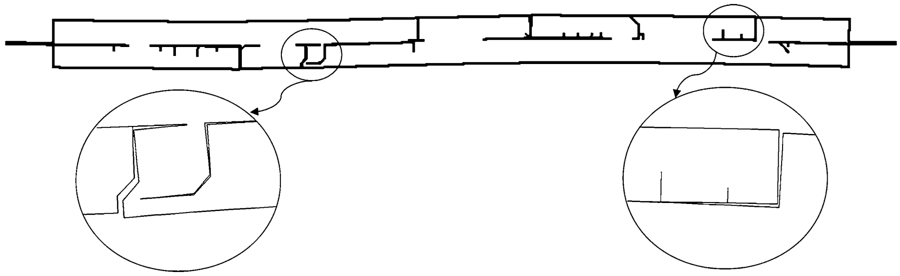

Fig. 13 Cracking profile for tie-beam numerical simulation at 30 kN (cracks over 300 μm)

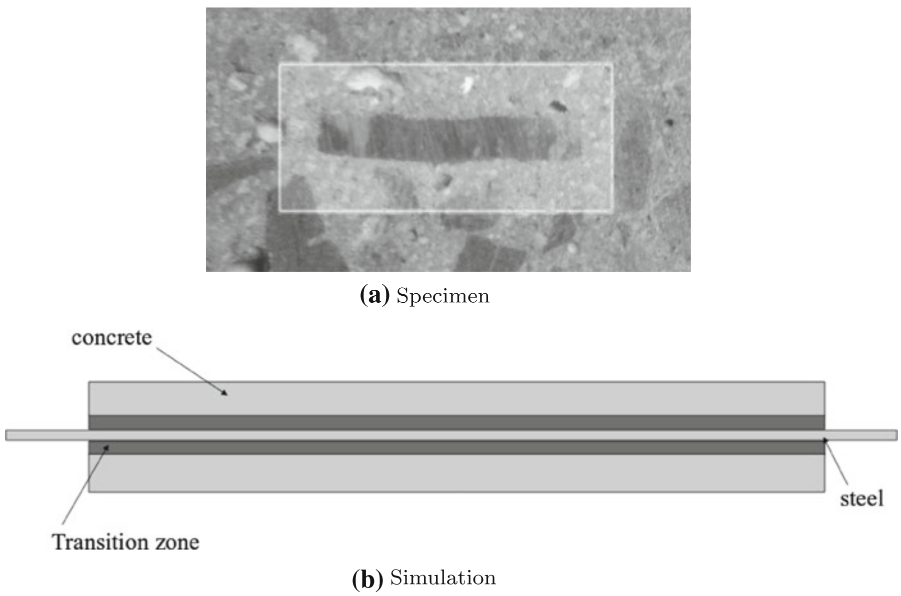

Fig. 14 Transition zone around the steel

  – Two sensors (LVDTs 5, 6) are located on the steel rebars, on both extremities of the tie beam.

- For the measure of the concrete elongation:
  – Two sensors (LVDTs 1, 3) are located on one face of the tie-beam with a base length of 150 cm.
  – Two other sensors (LVDTs 2, 4) are located on the opposite face of the tie-beam with the same base length of 150 cm.

mable support independent of the specimen.

As a consequence, each couple of LVDTs provides the measurement of a relative displacement (of the steel and of the concrete). The six displacement sensors and the two load sensors are connected to a central acquisition system where the information is automatically recorded.

5.2 Concrete and steel reinforcement

The concrete used in these tests is a B40/50. Its design is reported in Table 1.

To determine the material characteristics of the concrete, compressive tests were performed on standardized (French standard) cylindrical specimens (160 mm in diameter and 320 mm high). It must be noticed that the compressive tests were performed at the same age as the tie-beam tests and under the same conditions of preservation.

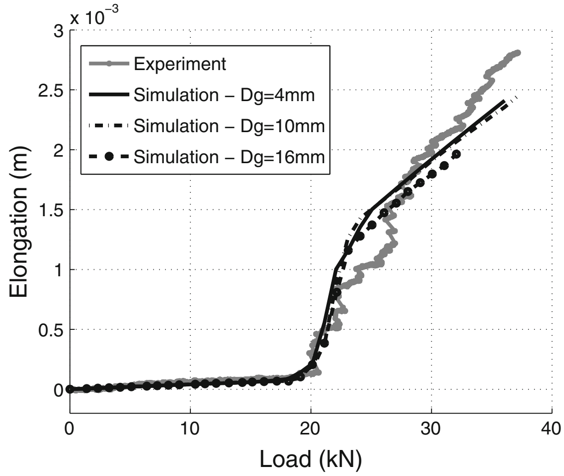

(a) Relative displacement

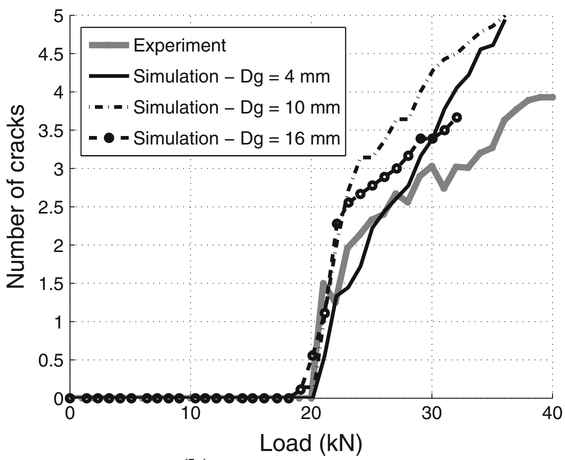

(b) Number of cracks

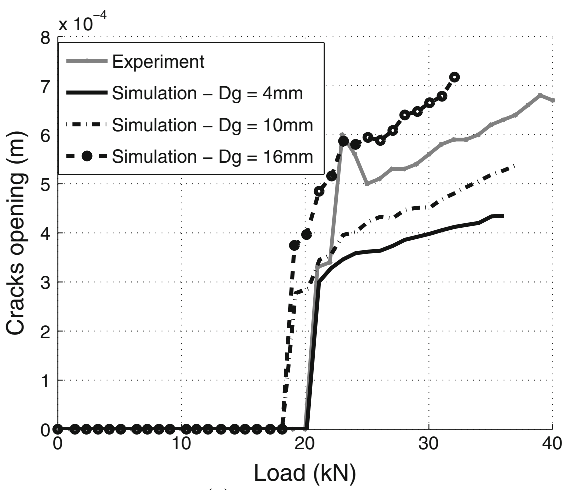

(c) Cracks opening

Fig. 15 Numerical results related to the effect of the transition zone surrounded steel

Table 2 presents the material characteristics of the concrete and of the flat steel.

5.3 Strategy of analysis of the test results

A strategy of analysis of the tests results is proposed to get a consistent method to analyse the experimental test results and the simulations ones. Table 3 presents the parameters retained for this analysis of the global and local behaviours in both cases, experiment and modeling.

Each parameter is recorded in function of the applied load. The following lines describe how these parameters are obtained in practice:

5.3.1 Determination of the mean crack opening

- A crack is counted if it is seen across an entire width of one side of the specimen, i.e. two adjacent edges are open. The opening of this crack is equal to the average of the openings related to the adjacent edges. For example, in Fig. 9, Face 1 presents two opened adjacent edges ($w_1 \geq 0$ and $w_2 \geq 0$); a crack is then counted, having a width given by:

$$w = \frac{w_1 + w_2}{2}$$

and Face 2 presents only one opened ($w_2 \geq 0$); then no crack is counted on this face. For this kind of test, and according to Eurocode 2[3] in the case of RC structures, a crack is considered only if its opening w is equal to or higher than 300 μm (value which corresponds to prejudicial crack opening for service limit states).

- For each face, the average of all cracks openings (if cracks are counted on this face) is computed.
- The final mean value of the cracks opening of the tie-beam is given by the average of the preceding mean values (if it exists) obtained for each face.

5.3.2 Determination of the the number of cracks and cracks spacing

- The same strategy is adopted.

[3] Eurocode 2—design of concrete structures.

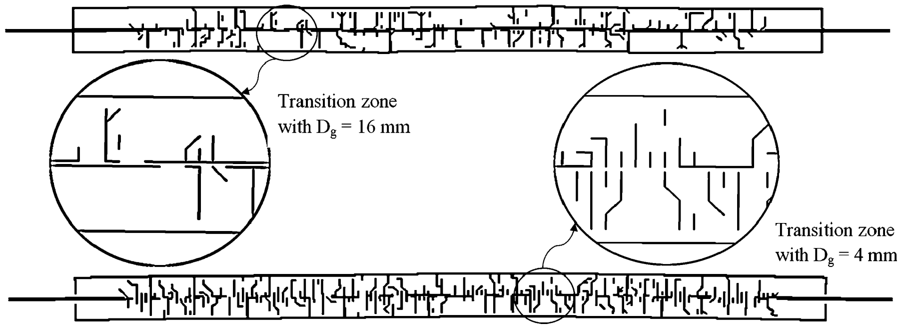

Fig. 16 Cracking pattern around the interface zone for different size of aggregate

Fig. 17 Eccentricity of the steel rebar

Note that this strategy of analysis of results can be performed on the 3D experimental test configuration as well as on the one of the 2D modeling. Although this strategy only considers cracks of openings $\geq$300 μm, the model is able to describe smaller crack openings. They are not taken into account in this analysis.

5.4 Numerical simulations: parametric study

In this section, the experimental tie-beam tests are numerically simulated. The work consists in identifying the values of the parameters of the steel-concrete behaviour interface by an inverse analysis approach. The numerical results are compared with the experimental ones.

The mesh adopted for the numerical simulations is given in Fig. 10, and as already mentioned, the simulations are 2D ones.

In this work, the concrete is modeled in the frame of the probabilistic discrete cracking model described above. The steel remains elastic as far as only the service limit state is considered. The steel-concrete bond is represented by interface elements located along the steel. The values of the damage model parameters (the cohesion C and the critical tangential relative displacement δ_t^{cri}) describing the behaviour of this interface have to be determined (it is the objective of the inverse approach).

The parametric study is realized by varying the cohesion C (10, 15, 20, 25, 30 MPa) and the critical tangential relative displacement δ_t^{cri} (δ_t^e, 3, 6, 10, 30 μm) of the steel-concrete interface behaviour. In order to compare numerical simulations to experiments, nine simulations per configuration have been performed by using a Monte-Carlo method (each simulation corresponding to one random distribution of mechanical properties in the concrete). A total of 225 calculations have been performed for this parametric study.

Material characteristics used in the numerical simulation are presented in Table 4. The value of δ_t^e is calculated from the equation (5) and depends directly on the value of C (for example, with C = 10, the value of δ_t^e is $10/k_t$).

5.5 Numerical results and comparison with experiments

The numerical results of the parametric study have been analyzed in the same way than those related to the experiments (detailed in Sect. 5.3). The comparison has been made at the global level (load vs. displacement curves, Figs. 11a, 12a) and also at a local level (analysis of the cracking: number of cracks, cracks openings and cracks spacing vs. load, Figs. 11b–d, 12b–d).

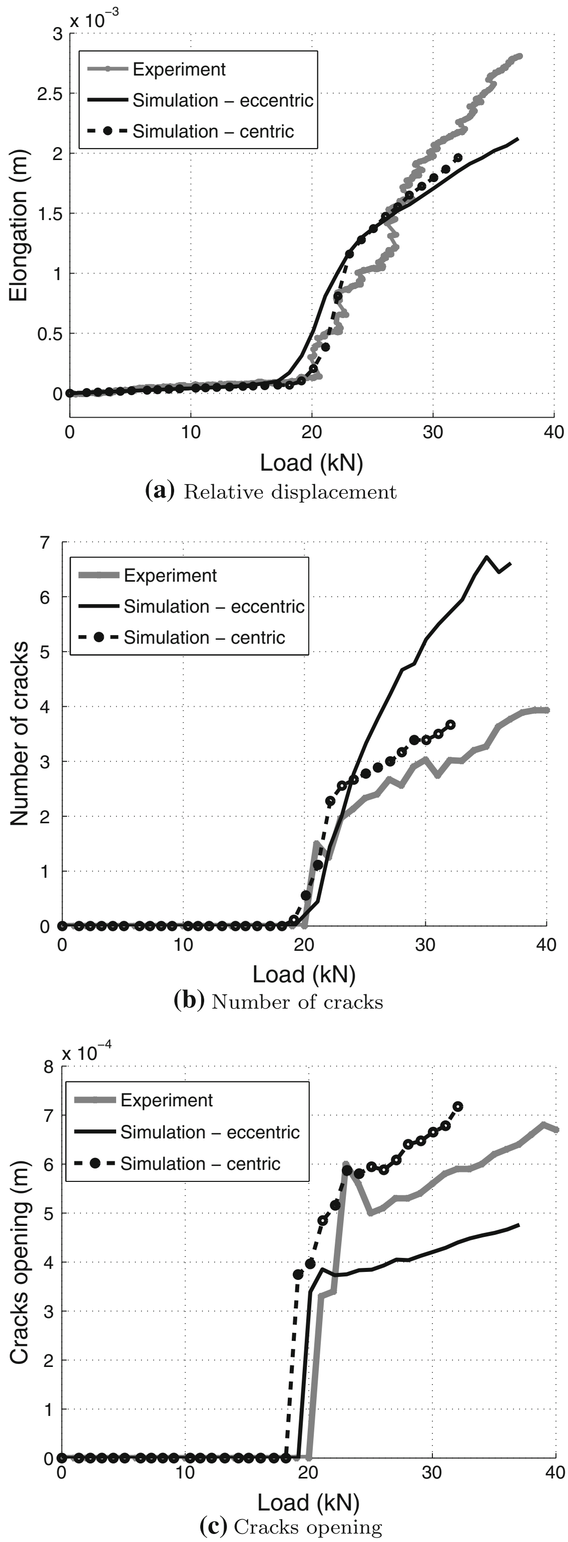

Fig. 18 Results on the effect of the eccentricity of steel

It is recalled that only cracks of an opening greater than or equal to 300 μm are considered. The analysis of the numerical results follows the strategy developped in Sect. 5.3 (the same procedure was used for the experimental results).

The comparison of these results with the experiment leads to distinguish that the couple of parameters, C = 10 MPa and δ_t^{cri} = 10 μm, gives the best results. Results of the comparison are shown in Figs. 11 and 12 for this couple of parameter. The numerical curves are in black bold, and the experimental curves are in grey. In terms of average values, as well as in terms of scattering (for nine computations and nine tests), the obtained curves have almost identical profiles. However we can note that the cracks appear slightly earlier in numerical simulations (see Fig. 11a–d).

Figure 12a shows the scattering of elongation (maximum and minimum values) related respectively to the experience and the simulations. The same analysis on the cracking process is synthesized in Figs. 12b–d.

These results clearly show that the numerical approach is efficient to represent the global response as well to give information about cracking process related to the tie-beam behaviour in tension. One can however observe that these results are obtained in the rough assumption of a 2D simulation of the experiment.

Figure 13 presents an example of the numerical cracking profile of the test on the tie-beam, showing explicitly the cracks and its development. This result is obtained at a load of 30 kN.

5.6 Influence of the eccentricity of the bar and of the transition zone around the steel

The model remains an idealized view of the reality. Some factors may potentially play a non negligible role in the structural behaviour. Two factors have been studied here: the internal structuration of the concrete near the rebar and the eccentricity of the steel reinforcement.

5.6.1 Effect of the internal structuration of the concrete

On the tested specimens, a zone around the flat steel, where the granulometry is finer than in the current zones, was observed (Fig. 14a).

The mechanical properties of this region are more homogeneous than other parts of the concrete. Zones of concrete of different natures can be represented around the steel in the numerical simulations (see Fig. 14b). Two additional series with different maximum aggregates size, $D_g = 4$ mm and $D_g = 10$ mm, in the transition zone at the surrounding of the steel reinforcement, were simulated. The results are presented in Fig. 15a–c.

The results show that the effect of a lower heterogeneity in the transition zone does not really influence the global response of the tie beam (Fig. 15a). But, it clearly influences the openings of macrocracks which decrease significantly with a decrease of the maximum aggregates size (Fig. 15c). A slighter effect on their number is also observed (Fig. 15b). As a consequence, the more the transition zone is homogeneous, the more it is microcracked: the cracking is better diffused in the surrounding concrete (see Fig. 16).

5.6.2 *Effect of the eccentricity*

In the case of the specimen (Fig. 17), an eccentricity of about 10 mm was observed. To quantify the influence of this eccentricity, a series of numerical simulations have been performed by taking into account a constant eccentricity of 1 cm of the steel rebar. Of course, a constant eccentricity can only be a poor approximation of the reality.

The analysis of the results leads to the following remarks: a slight difference between both cases, centered and eccentered, when the global response is concerned (Fig. 18a) and significant ones in terms of numbers or openings of cracks (Fig. 18b, c) allow to conclude that, in the case of the eccentered rebar:

- Macrocracks appear later (Fig. 18b, c),
- But many microcracks, leading to a greater elongation of the concrete, appear earlier at the interface (Fig. 18a).

As an evidence, the essential of the cracking appears mainly on the side where the cover is the smallest.

6 Conclusions

A simple model for describing the behaviour of the interface between concrete and steel in RC structures members is presented. Coupled with an explicit probabilistic cracking model for the concrete behaviour, this model is used to simulate the mechanical behaviour of a tie-beam subjected to tension. Its parameters, related to the use of flat steel reinforcement, have been determined through an inverse approach. In the frame of a 2D analysis, the interface model with two parameters (C, δ_t^{cri}) developed in relation with a probabilistic discrete cracking model (for concrete), seems to give good results in comparison with experiment. If a 3D analysis was used, it is clear that the values of the parameters (of the interface model) determined in the frame of the inverse approach performed in this study would have been different. The model can provide relevant information on the cracking process (cracks opening and spacing) even at smaller scale compared to what can be experimentally determined.

It must be emphasized that the effect of the existing transition zone between steel and concrete as well as the observed eccentricity of the rebar position are difficult to take into account in the frame of the numerical simulations. Nevertheless, a parametric study has allowed to determine a trend of their effects on both global and local results.

The behaviour of the steel-concrete interface is mainly related to (1) the shape of the surface of the rebar and (2) the type of concrete used. The presented methodology can be used to determine the model parameters for different couples of reinforcement and concrete and the resulting set of parameters can then be used to simulate the behaviour of any concrete structures using these types of concrete and reinforcement.

Acknowledgements Thank you to Mr. Henry Thonier and Mr. Daniel Constantin, advisors, for their contributions and comments. We would also appreciate the financial support of the construction company MATIERE®.

References

1. Rossi P, Wu X (1992) A probabilistic model for material behaviour analysis and appraisement of concrete structures. Mag Conc Res 44(161):271–280
2. Rossi P, Wu X, LeMaou F, Belloc A (1994) Scale effects on concrete in tension. J Mater Struct 27(172):437–444
3. Tassios TP (1979) Properties of bond between concrete and steel under load cycles idealizing seismic action. Bull d'information du CEB 131:65–122
4. Romdhane MRB, Rossi P, Ulm FJ (1999) The steel-concrete interface revisited: micro-mechanical analysis. Concr Sci Eng 1:215–221

5. Ozbolt J, Eligehausen R (1992) Numerical simulation of cycling bond-slip behaviour. In: Proceedings of international conference on Bond in Concrete CEB, pp 12.27–12.33
6. Cox JV, Herrmann LR (1998) Development of a plasticity bond model for steel reinforcement. Mech Cohesive-Frict Mater 3:155–180
7. Rots JG (1988) Computational modeling of concrete fracture. Ph.D. Dissertation, Delft University of Technology, Delft
8. Reinhardt HW, Blaauwendraad J, Vos E (1984) Prediction of bond between steel and concrete by numerical analysis. Mater Struct 17(100):311–320
9. Lundgren K (2005) Bond between ribbed bars and concrete. Part Charact 1: modified model. Mag Concr Res 57(7):371–382
10. Cox K (1999) Computational models for the bond between FRP reinforcing bars and concrete. American Society of Composites, 14th Annual Technical Conference Dayton, OH
11. Cox JV, Guo J (2000) Implementation of a plasticity bond model for reinforced concrete. Comput Struct 77:65–82
12. Herrmann LR, Cox JV (1994) Development of a plasticity bond model for reinforced concrete: preliminary calibration and cyclic applications. Contract Report CR 94.001-SHR, Naval Facilities Engineering Service Center Port Hueneme, CA
13. Cox JV, Herrmann LR (1999) Validation of a plasticity bond model for steel reinforcement. Mech Cohesive-Frict Mater 4:361–389
14. Richard B, Ragueneau F, Cremona C, Adelaide L, Tailhan J-L (2010) A three-dimensional steel/concrete interface model including corrosion effects. Eng Fract Mech 77(6): 951–973
15. Ragueneau F, Dominguez N, Ibrahimbegovic A (2006) Thermodynamic-based interface model for cohesive brittle materials : application to bond slip in RC structures. Comput Methods Appl Mech Eng 195:7249–7263
16. Willam K, Rhee I, Shing B (2004) Interface damage model for thermomechanical degradation of heterogeneous materials. Comput Fail Mech 30–32(193):3327–3350
17. Raous M, Cangémi L, Cocu M (1998) A consistent model coupling adhesion, friction, and unilateral contact. Comput Methods Appl Mech Eng 177(1999):383–399
18. Simons JW, Bergan PG (1986) A finite element formulation of three-dimensional contact problems with slip and friction. Comput Mech 1:153–164
19. Talon C, Curnier A (2003) A model of adhesion coupled to contact and friction. Eur J Mech A Solids 22:545–565
20. Frémond M (1987) Adhérence des solides. J Méc Théor Appl 6(3):383–407
21. Frémond M (1988) Contact with adhesion. In Moreau J-J, Panagiotopoulos PD (eds) Nonsmooth mechanics and applications, CISM Courses and Lectures, vol 302. Springer, Wien, pp 177–221
22. Rossi P (1993) Comportement dynamique des bétons: du matériau la structure, Annales de l'Institut technique du bâtiment et des travaux publics, No 511
23. User manual (1994) Module TACT, 3rd edn. CESAR-LCPC
24. De Soza T (2012) Notice d'utilisation du contact, Fascicule u2.04: Mécanique non linéaire, Révision 8205, Code_Aster v10